

## TIME DELAYS

T. WIKLIND

*Onsala Space Observatory, SE-43992 Onsala, Sweden*

The present status of measured time delays in gravitational lens systems and the analysis methods are presented. The use of molecular absorption lines to derive the time delay in PKS1830-211 is discussed. Finally, an assesment is made of how accurate the Hubble parameter  $H_0$  can be derived and where the major uncertainties remain.

### 1 Background

Until just a few years ago, there was only one gravitational lens where observers had attempted to derive the differential time delay. Today this situation is rapidly changing, with time delays for 7 lenses published and with several in the process of being observed.

The idea of using the differential time delay between two or more images of a lensed background source to determine the value of the Hubble parameter,  $H_0$ , was around for more than 15 years before the first gravitational lens, Q0957+561, was discovered (Refsdal 1964; Walsh et al. 1979). Q0957+561 turned out to be variable and the first attempts to measure the time delay started almost immediately. Several different methods were used, from radio interferometry (including VLBI) to optical photometry (for list of early attempts, see Haarsma et al. 1997). The results quickly divided themselves into a 'high-value' and a 'low-value' group, where the high value corresponded to  $\Delta t \approx 540 \pm 10$  days and the low value to  $\Delta t \approx 410 \pm 20$  days. These discrepant results emerged because the two lens components do not vary in the same way. This is most likely due to microlensing in the intervening galaxy, but also because derivation of the time delay is intrinsically difficult. In principle, it is a classical problem, the correlation of two unevenly sampled time series, but with the added complexity that the two time series are not sampled simultaneously.

In order to use the differential time delay for cosmography, it is necessary to have a well determined gravitational potential of the lensing galaxy, as well as the redshifts of both the lens and the background source. With these ingredients, the time delay effectively measures the distance between the two points for which the arrival time difference has been determined. With the known angular separation on the sky, one obtains the angular size distance, independent on any other cosmological distance measurement. This is of course a function of the Hubble parameter  $H_0$ , but also  $\Omega_0$  and  $\Omega_\Lambda$ , the density parameters for matter and a cosmological constant. Hence, a time delay measurement, with a well constrained potential, defines a surface in a multiparameter space ( $H_0, \Omega_0, \Omega_\Lambda$ ). Measurement of differential time delays from several gravitational lenses, at different redshift combinations of the lens and the source, can in principle be used to solve simultaneously for all the parameters. This is presently not feasible due to uncertainties in the lens potentials.

Table 1: Time delay measurements as of March 2000

Name	$z_d$	$z_s$	$\Delta t$ days	$\sigma_{\Delta t}/\Delta t$	Method	Ref.	
B0218+357	0.68	0.96	$10.5^{+0.4}_{-0.4}$	4%	Radio (polarimetry)	Biggs et al. 1999	
Q0957+561	0.36	1.41	$409^{+23}_{-23}$	6%	Radio	Pelt et al. 1994	
			$423^{+6}_{-6}$	1%	Optical	Pelt et al. 1996	
			$417^{+3}_{-3}$	1%	Optical	Kundic et al. 1997	
			$425^{+17}_{-17}$	4%	Optical	Pijpers 1997	
			$397^{+20}_{-20}$	5%	Radio	Haarsma et al. 1997	
			$409^{+30}_{-30}$	7%	Radio	Haarsma et al. 1999	
HE1104-1805	0.77	2.32	$267^{+7}_{-7}$	—	Spectrophotometry	Wisotzki et al. 1998	
PG1115+080	0.31	1.72	CB	$23.7^{+3.4}_{-3.4}$	14%	Optical	Schechter et al. 1997
			A1A2	$9.4^{+2}_{-2}$	—		
			CB	$25.0^{+3.3}_{-3.8}$	14%	Optical	Barkana 1997
B1600+434	0.42	1.59	$47^{+12}_{-9}$	23%	Radio	Koopmans et al. 2000	
B1608+656	0.63	1.39	BA	$26^{+5}_{-5}$	19%	Radio	Fassnacht et al. 1999
			BC	$34^{+5}_{-5}$	15%		
			BD	$73^{+5}_{-5}$	7%		
PKS1830-211	0.89	2.51		$44^{+9}_{-9}$	20%	Radio	van Onnen et al. 1995
				$26^{+4}_{-5}$	17%	Radio	Lovell et al. 1998
				$28^{+4}_{-4}$	14%	Millimetric	Wiklind et al. 2000

## 2 Present status

At the time of writing, time delays have been derived for 7 gravitational lenses, summarized in Table 1. Data for one additional lens (B1422+231) is discussed in these proceedings (Narashima). Some of the values are still rather uncertain, as can be seen from the  $\sigma_{\Delta t}/\Delta t$  values in Table 1. The best ones correspond to fractional errors of only a few percent, while some values do not even have estimates of the uncertainties. Typical uncertainties, at the  $\sim 90\%$  confidence limit, is 10-20%. The lens with the best estimated time delay is Q0957+561, where time series extending over more than 20 years exist.

Of the seven lenses listed in Table 1, four have been observed at radio wavelengths (including the millimeter band), two in optical bands and one (Q0957+561) at both radio and optical wavelengths. This dominance of radio observations is due to large gravitational lens surveys like CLASS, which have been more successful than optical surveys in finding new lenses. Moreover, the CLASS survey is biased towards flat spectrum radio sources, likely to be beamed towards us and therefore more variable than less beamed sources.

The redshift for the lens in HE1104-1805 remains undetermined and this source can not be used for cosmographic purposes - yet. It also has one of the most uncertain time delays. The remaining six sources have all been used to get estimates of  $H_0$  (see below).

Interestingly, three of the six sources where reasonably good time delay measurements exist, are late type galaxies. This is seen either through morphology (B1600+434) or through detection of molecular gas (B0218+357 and PKS1830-211). It remains to be seen whether this implies that the potentials used for the lens modelling should be modified.

There are still a number of gravitational lens systems detected in the CLASS survey which can be used to derive differential time delays, but for which data do not exist at the moment: B1933+503, where Biggs et al. (2000) found little variability during a monitoring campaign in 1998, and B1030+074, which is presently being monitored (Xanthopoulos et al. 2000).

The gravitational lens PKS1830-211 and the  $z=0.89$  absorption line system

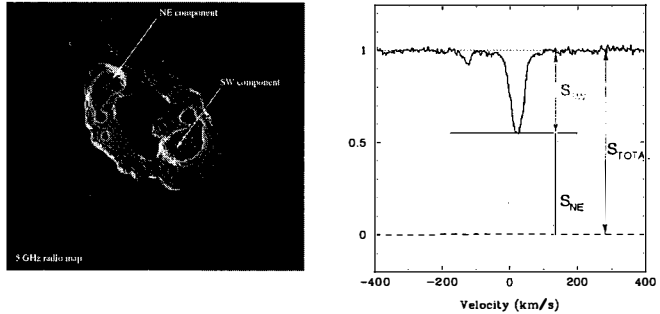


Figure 1: *Left:* A 5 GHz image of PKS1830-211 (courtesy A. Patnaik). The cores, which are the only parts contributing to the continuum at millimeter wavelengths are marked. *Right:* The  $\text{HCO}^+$  (2-1) spectra at  $z = 0.89$  observed with the SEST. The line is saturated and only covers the SW component.

### 3 Methods

The controversy regarding the time delay for Q0957+561 underlined the difficulties associated with deriving a  $\Delta t$  value from an unevenly sampled time series. It also motivated several groups to design analysis methods appropriate for this type of data.

Apart from correlating unevenly sampled time series, gravitational lenses provide the extra complication that the series are effectively sampled at different times. There are three ways to attack this type of problem: (1) interpolate unobserved data points and use conventional correlation techniques, (2) bin observations to get uniformly spaced data (using uneven window functions) and use conventional correlation techniques, or (3) use what you have and try to correlate as best as possible. The last method has been developed by Pelt et al. (1994; 1996) with the special goal of analysing the time delay for Q0957+561. It is a nonparametric method which is essentially a cross-correlation, but where the correlation is done with the nearest neighbouring data point (in time). This method has become known as the ‘Pelt Dispersion Method’. An elaborate method for optimizing the interpolation between data points has been developed by Press et al. (1992a,b), again with the goal of deriving the time delay of Q0957+561. Edelson & Krolik (1988) developed a discrete cross-correlation method, aimed for analysis of reverberation mapping of AGNs, which can be used for gravitational lens time delays. The method optimizes the binning (rather than the interpolation) and requires a fairly well sampled data set to retain sufficiently good temporal resolution. In the literature one can find several other techniques that have been developed for gravitational lenses (cf. Pijpers 1998; Barkana 1997, 1999).

Since almost all of these methods have been developed with analysis of the time delay of Q0957+561 in mind, it is fortunate that the controversy arised for this particular source.

### 4 Using molecular absorption lines: PKS1830-211

A new method for monitoring the fluxes from gravitational lens systems has originated with the detection of molecular line absorption in intervening galaxies (cf. Wiklind & Combes 1995, 1996). The centralized distribution of molecular gas implies that whenever absorption is detected, the background continuum source has an impact parameter of a few kpc or less. This is an ideal situation for strong lensing.

A total of four molecular absorption line systems has been detected, with redshifts in the range  $z = 0.25-0.89$ . Two of these occur in lensing galaxies: B0218+357 ( $z_d = 0.68$ ) and

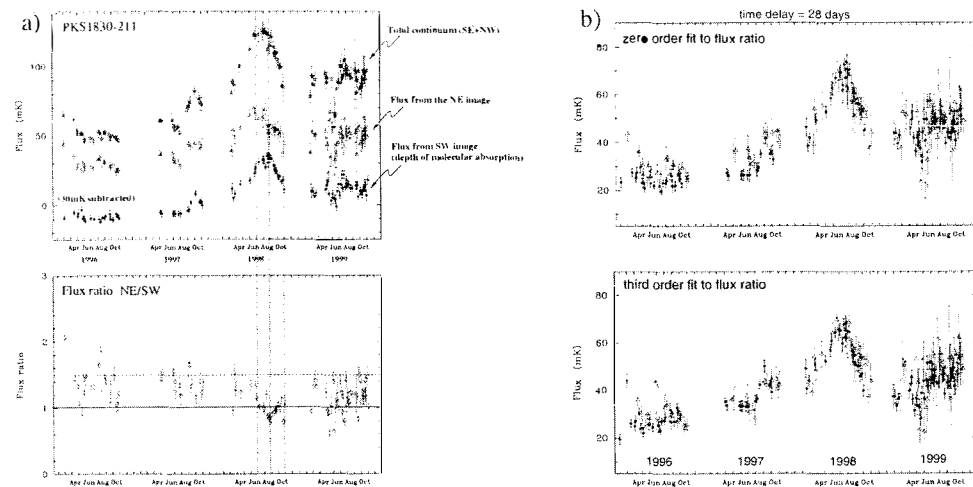


Figure 2: Monitoring of PKS1830-211. **a)** The top panel shows the data obtained over 4 years. The bottom panel shows the flux ratio of the NE and SW components. A clear signature of the time delay between the NE and SW images can be seen during the peak of the outburst in 1998. **b)** The fluxes from the NE (gray) and SW (blue/black) components. The SW component has been shifted by  $\Delta t = -28$  days. In the upper panel the components are shown for a constant magnification ratio ( $\mu = 1.3$ ), while the lower panel shows the result when a third order polynomial has been fitted to the magnification ratio when solving for  $\Delta t$ . The latter case represents a much better solution.

PKS1830-211 ( $z_d = 0.89$ ). In both cases, the absorbing molecular gas obscures one of two images. Several different molecular transitions have been observed and some of them are strongly saturated. This is seen through the detection of isotopic species, for instance  $\text{HCO}^+$  and the isotopic variants  $\text{H}^{13}\text{CO}^+$  and  $\text{HC}^{18}\text{O}^+$ . While the continuum flux at frequencies off an absorption line gives the sum of the fluxes from the images, the depth of a saturated absorption line gives the flux from the obscured image. This can be used to monitor the individual fluxes without actually resolving them. For instance, in PKS1830-211 the separation between the images (see Fig. 1) is  $\sim 1''$ , but the fluxes of the individual images can be obtained with a telescope with an angular resolution of  $\sim 50''$ .

Fig. 1 shows PKS1830-211 at radio wavelengths (courtesy A. Patnaik), showing two images with a core+jet morphology. The jet has a steep spectral index and at millimeter wavelengths only the inner cores contribute to the observed continuum. The strong absorption occurs towards the SW component (Wiklind & Combes 1998). Due to heavy Galactic extinction the system can only be detected at wavelengths longer than a few microns. The saturated  $\text{HCO}^+(2-1)$  transition occurring at  $z = 0.89$  towards PKS1830-211, also shown in Fig. 1, has been monitored with the SEST 15m telescope at La Silla since April 1996 (Wiklind & Combes 2000). During this time the total flux has varied by a factor  $\sim 2.5$  (Fig. 2a). During an outburst in 1998, we detected a clear signal of time delay, which can be seen in the flux ratio of the NE and SW components in Fig. 2a. Analysis of the complete dataset using several different methods, gives a time delay  $\Delta t = 28^{+4}_{-4}$  days, with the NE component leading. The results of Lovell et al. (1998), based on low frequency interferometric techniques and model subtraction of the jet components, gives a time delay of  $\Delta t = 24^{+5}_{-4}$  days. These two measurements have completely different sets of possible systematic errors and the good agreement gives additional confidence to the results. Using the lens model of Nair et al. (1993), our time delay corresponds to  $H_0 = 59^{+9}_{-11} \text{ km s}^{-1} \text{ Mpc}^{-1}$ .

The best fit for the molecular data is given by  $\Delta t = 28$  days. However, solving for a constant magnification ratio, gives a time dependent offset between the rectified fluxes from the NE and

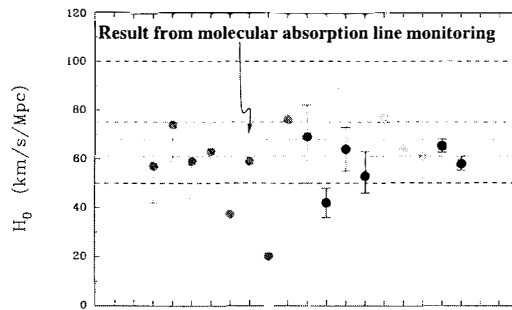


Figure 3: Derived values of  $H_0$  using time delays. The values are taken from the literature and various types of lens potentials have been used in the modelling, from parametrized models to nonparametric ones. Green/gray points represent results based on radio data, blue/black point optical data and light blue/grey Q0957+561 (combined radio and optical). Although the dispersion is large,  $\sim 80\%$  of the values are within the uncertainty quoted in the HST Key Project on the Extragalactic Distance Scale, as marked by dot-dashed lines. The two black points to the right represent  $H_0$  values derived from NGC4258; one using water masers and the other using cepheids.

SW components (Fig. 2b). This suggests that a long term variation of the magnification ratio is taking place. A better fit can be achieved by letting the flux ratio vary as a third order polynomial (Fig. 2b). The time scale for this variation is 1-2 years. The size of the background source at millimeter wavelengths is unknown, but likely to be of the order  $10^{17}$ - $10^{18}$  cm. Although this is large for microlensing events, this remains a possible explanation for the long term variation. A further complication here is that the background source could exhibit superluminal motion and it is not only the foreground screen that has a transverse velocity. We hope to follow this source in order to follow up on the behaviour of the magnification ratio.

## 5 Prospects for deriving $H_0$

Various estimates of the Hubble parameter using time delays, taken from the literature, are shown in Fig. 3. The dispersion of values is quite large. Differential time delay measures the angular size distance, with  $H_0$ ,  $\Omega_0$  and  $\Omega_\Lambda$  as parameters. The strongest dependence, however, is on the Hubble parameter and it is common to set  $\Omega_0 = 1$  and  $\Omega_\Lambda = 0$  and quote a value for  $H_0$ . This has been done for the values shown in Fig. 3 and some of the dispersion could be caused by parameter having intrinsic values different from the assumed ones. However, the strongest cause for the dispersion comes from the different types of lens models used. The number of  $H_0$  values presented in Fig. 3 is almost three times the number of lenses with known time delay. Some values of  $H_0$ , derived for the same lens system with the same  $\Delta t$ , gives results which are inconsistent with each other. This shows that the main uncertainty remains in the lens modelling. Nevertheless, in this ‘pessimistic’ view, 80% of the  $H_0$  values are consistent within the uncertainty quoted in The HST Key Project on the Extragalactic Distance Scale (Mould et al. 2000). A much smaller dispersion of  $H_0$  values, based on time delay measurements, can be achieved by using the same type of lens models for all sources (cf. Koopmans & Fassnacht 1999). However, possible systematic errors could be introduced in this manner.

## Acknowledgments

We (Françoise Combes and I) thank the SEST Team for expert help in doing the monitoring of PKS1830-211 during a long time period.

## References

1. Barkana R., et al., ApJ **520**, 479 (1999)
2. Barkana R., ApJ **489**, 21 (1997)
3. Biggs A.D., Xanthopoulos E., Browne I.W.A., Koopmans L.V.E., Fassnacht C.D., MNRAS, in press (2000) astro-ph/0004290
4. Biggs A.D., et al., MNRAS **304**, 349 (1999)
5. Edelson R. A., Krolik, J. H., ApJ **333**, 646 (1988)
6. Fassnacht C.D., et al., ApJ **527**, 498 (1999)
7. Haarsma D.B., Hewitt J.N., Lehar J., Burke B.F., ApJ **510**, 64 (1999)
8. Haarsma D.B., Hewitt J.N., Lehar J., Burke B.F., ApJ **479**, 102 (1997)
9. Koopmans L.V.E. & de Bruyn A.G., A&A **358**, 793 (2000)
10. Koopmans L.V.E., de Bruyn A.G., Xanthopoulos E., Fassnacht C.D., A&A **356**, 391 (2000)
11. Koopmans L.V.E. & Fassnacht C.D., ApJ **527**, 513 (1999)
12. Kundic T., et al., ApJ **482**, 631 (1997)
13. Lovell J.E.J., et al., ApJ **508**, L51 (1998)
14. Mould J.R., et al., ApJ **529**, 786 (2000)
15. Nair S., Narasimha D., Rao A.P., ApJ **407**, 46 (1993)
16. Pelt J., Kayser R., Refsdal S., Schramm T., A&A **305**, 97 (1996)
17. Pelt J., Hoff W., Kayser R., Refsdal S., Schramm T., A&A **286**, 775 (1994)
18. Pijpers F.P., Ap&SS **261**, 337 (1998)
19. Press W.H., Rybicki G.B., Hewitt J.N., ApJ **385**, 404 (1992a)
20. Press W.H., Rybicki G.B., Hewitt J.N., ApJ **385**, 416 (1992b)
21. Refsdal S., MNRAS **128**, 370 (1964)
22. Schechter P., et al., ApJ **475**, L85 (1997)
23. van Ommen T.D., Jones D.L., Preston R.A., Jauncey D.L., ApJ **444**, 561 (1995)
24. Walsh D., Carswell R.F., Weymann R.J., Nature **279**, 381 (1979)
25. Wiklind T., Combes F., 2000, in *Gravitational Lensing: Recent Progress and Future Goals*, Boston University July 1999, eds. T.G. Brainerd, C.S. Kochanek, astro-ph/9909314
26. Wiklind T., Combes F., ApJ **500**, 129 (1998)
27. Wiklind T., Combes F., Nature **379**, 139 (1996)
28. Wiklind T., Combes F., A&A **299**, 382 (1995)
29. Wisotzki L., Wucknitz O., Lopez S., Sorensen A.N., A&A **339**, L73 (1998)
30. Xanthopoulos E., et al., 2000, in *Gravitational Lensing: Recent Progress and Future Goals*, Boston University July 1999, eds. T.G. Brainerd, C.S. Kochanek, astro-ph/9909460